EXPLORING THE SOUTH MASSIF of the TAURUS-LITTROW VALLEY (TLV) BY EXAMINING THE LESS THAN 2mm LITHIC FRAGMENTS IN THE 73001/73002 DOUBLE DRIVE TUBE. S.B. Simon[1,2], C.K. Shearer[1,2,3], M. Cato[2,4], B.L. Jolliff[5], C. Neal[6], J.J. Papike[1,2], and the ANGSA Science Team. [1]Institute of Meteoritics, University of New Mexico (UNM), Albuquerque, NM 87131, USA. [2]Department of Earth and Planetary Sciences, UNM, Albuquerque, NM 87131, [3]Lunar and Planetary Institute, Houston TX 77058; [4]Center for Stable Isotopes, UNM, Albuquerque, NM 87131; [5]Washington Univ. in St. Louis, St Louis, MO 63130; [6]Univ. of Notre Dame, South Bend, IN 46556. (sbs8@unm.edu)

Introduction: The double drive tube core sample (73001/73002) that was collected at Station 3 during the Apollo 17 mission penetrated a lunar landslide deposit that transported material from the slope of the South Massif into the TLV (Fig. 1). A valuable exploration and sampling feature of landslides on planetary surfaces is that they provide samples from terrains inaccessible to either human or robotic missions owing to steepness and safety concerns. The steep northeast slope of the South Massif (2200 m) of the TLV is a case in point. Orbital data suggest that the light mantle deposit associated with the South Massif represents multiple landslide events that were triggered by movement along the Lee-Lincoln scarp [e.g., 1] or impact events [e.g., 2]. Samples from Stations 2 and 3 [3-6] show that the light mantle constituents are very similar to those of the impact breccia-dominated regolith on the slope of the South Massif. From remotely collected FeO-TiO_2 contents of the light mantle deposit, [6] concluded that these materials are dominated by impact melt breccia of the types sampled at Station 2, but these compositions extend almost exactly from the granulitic lithologies toward a high-Ti basalt + orange volcanic glass component. They also noted that the South Massif is fairly heterogeneous with melt rock-rich surfaces on the north slope while the regolith on the southern slopes of South Massif reflects mixing with a basaltic component (e.g., impact ejecta from the surrounding basaltic plains, an older basaltic component). Jolliff et al. [5] illustrated some of the variability of lithic fragments and soils at the surface adjacent to the 73001/2 core. Lithic fragments from the 73002 greater than 4 mm in size were examined with XCT imaging. Valenciano et al. [7] illustrated the mineralogical and textural variation in three ilmenite basalt fragments from 73002 through the examination of XCT images. Lithic fragments smaller than 4 mm can make up an average of more than 8% of the total core and over 13% of some individual 0.5 cm core segments. These fragments have not been examined in detail. Here, we examine the mineral and textural variability of lithic fragments in the size range 2mm to 90µm with the purposes of fully understanding the material making up the South Massif and to identify potential new highland lithologies.

Analytical Approach: Samples received were from individual 0.5 cm segments of the core from the first dissection pass. All samples except the rind sample were sieved into two fractions during pass 1 curation (< 1 mm, >1mm). Larger sample masses were split for petrologic and stable isotope analysis (H, O, Cl, S), whereas small sample masses were used only for petrology. All samples designated for petrology were sieved into 5 size fractions: <20 µm, 20-90 µm, 90-150 µm, 150-250 µm, and 500-1000 µm. Only the rind sample was sieved for size fractions greater than 1 mm. The different size fractions were mounted on glass slides and polished for microbeam analysis. Two sections of 90-150 µm fractions (,163 and ,172) and one >1mm particle were examined. We collected backscattered electron (BSE) images and quantitative EDS analyses with a TESCAN Lyra3 SEM at the Univ. of New Mexico.

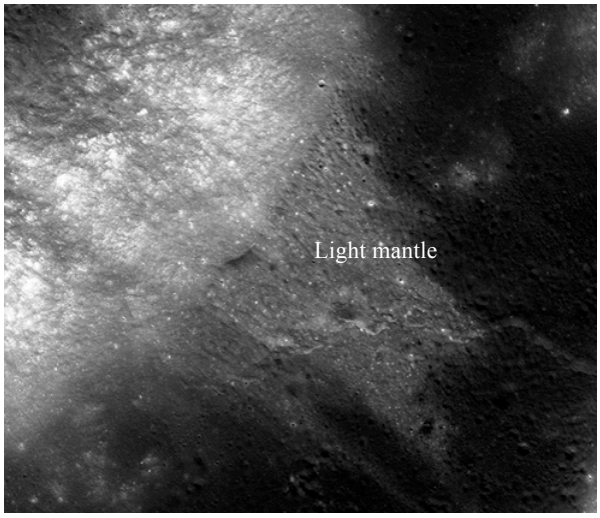

Fig. 1. LROC-NAC (Narrow Angle Camera) composite image of the TLV landslide deposit that includes the location of Station 3 and the 73001/2 core in the light mantle deposit, which is ~8 km across.

Results: In both soil sections studied, impact melt rocks are the most abundant, at 18.6 and 20.8% of the particles, followed by monomineralic plagioclase (16.9, 20.8%) in ,163 and ,172, respectively. Sample 163 has equal proportions of mare basalt and igneous highland rock fragments. Sample ,172 has smaller mare and larger highland lithic components than ,163. One >1 mm particle was examined (Fig. 2A). Lithic fragments in this breccia include several basalts; a melt rock; an anorthositic fragment with round olivine grains enclosed in plagioclase (Mg-suite); coarse, isolated plagioclase ($An_{91.2}$); and pigeonite ($En_{51.2}Wo_{21.8}Fs_{27.0}$) with fine exsolution lamellae [8].

Examples of lithic fragments found in the 90-150 µm fraction are shown in Fig. 2B-H. They include evolved mineral assemblages with intermediate plagioclase and zircon (Fig. 2B), crystalline melt breccias (CMB; Fig. 2C), basalts with a variety of textures and compositions (Fig. 2D,F,G), fragments with sodic feldspar-bearing mineral assemblages (e.g., Fig 2H; ilmenite + Cr-ulvöspinel + sodic plagioclase), and plutonic rock fragments (Fig. 2G).

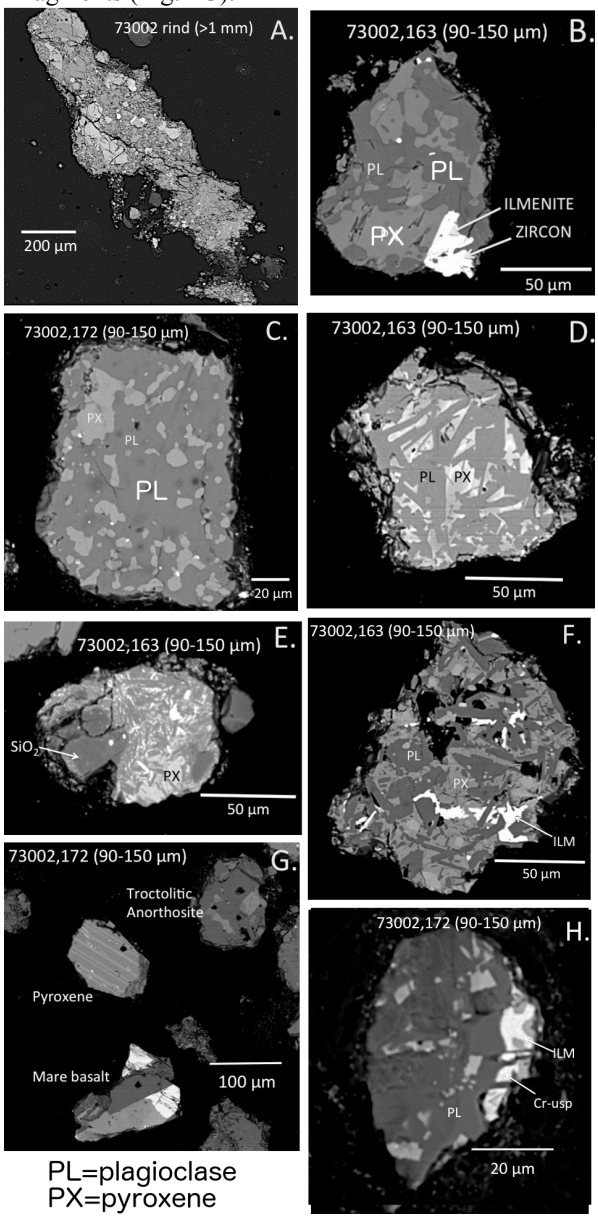

Fig. 2. Lithic fragments found in > 1mm and 90-150 µm size fractions in 73002. A. Regolith breccia. B. Assemblage of pyroxene + olivine + plagioclase + ilmenite + zircon. C. CMB. D. Feldspathic basalt. E. SiO_2-bearing lithology with pyroxene + intermediate plagioclase + ilmenite. F. Intermediate-Ti basalt. G. Three fragments. H. sodic feldspar (An_{42})-bearing fragment with ilmenite + Cr ulvöspinel.

Discussion: Although many of the lithic fragments in the <2 mm size fraction are similar to the coarser fragments identified by XCT imaging and analysis of surface materials collected on the landslide deposit, there are several distinctive lithologies.

Regolith breccias greater than 4 mm in size with a variety of lithic fragments have been identified through XCT in the 73002 core [8,9]. Similar textures and components are identified in the regolith breccia in Fig. 2A. Various melt rock lithologies are represented in surface material at Stations 2 and 3 [e.g., 1,3,4,6], and not surprisingly in 73002 as well. Examples of the latter include the olivine-pyroxene-plagioclase-zircon assemblage (Fig. 2B) and typical crystalline melt breccias (Fig. 2C). Nemchin et al. [10] reported zircon ages from the boulders at the base of South Massif ranging from 4.24 to 4.34 Ga. It is anticipated that zircons in the present samples have similar ages.

Small fragments of Mg-suite lithologies are also present. These are predominantly anorthosites, gabbros, and troctolites. In the landslide deposit, spinel is found in lithic fragments and as individual phases [e.g., 8]. As illustrated by Simon et al. [11] spinel is found in impact-produced lithologies as well as Mg-suite rocks. Lithic fragments and individual mineral phases such as SiO_2, intermediate-composition plagioclase ($\leq An_{50}$), K-feldspar ($An_1Ab_4Or_{95}$), Fe-rich pyroxene, and accessory zircon and Cr-ulvöspinel (e.g., Fig. 2B and H) represent evolved melts.

Based on the mineralogy of basalt fragments within the regolith and regolith breccias there appears to be considerable compositional variability. Basalt fragments include typical TLV high-Ti basalts (along with high-Ti pyroclastic glasses), high-Al basalts, and low-Ti basalts. This diversity implies a variety of basalt eruptions within and on the margins of the TLV. This is unlike the preliminary XCT examination of most of the >4 mm basalt fragments, which consist of high-Ti basalts with a limited range of cooling histories [7]. However, the initial assessment presented here must be considered preliminary, given the relatively small size and number of basalt fragments examined.

***References*:** [1] Schmitt H. (2017) *Icarus 298*, 2-33. [2] Lucchita B. et al. (1977) Icarus 30, 80-96. [3] Wolfe E. et al. (1981) *USGS Prof. Paper* 1080, p. 280. [4] Simon S. et al. (2020) Fall AGU abst. V013-0003. [5] Jolliff B. et al. (2020) Fall AGU abst. V013-0004. [6] Robinson M. & Jolliff B. (2002) *JGR: Planets*, *107*(E11), 20-1. [7] Valenciano J. et al. (2020) Fall AGU abst. V013-0003. [8] Cato M. et al. (2021) This vol. [9] Zeigler R. et al. (2020) LPSC 51 abst. #3023. [10] Nemchin A. et al. (2008) GCA 72, 668-689. [11] Simon S. et al. (2021) This vol.

***Acknowledgments*:** This work was funded by NASA through ANGSA grant **80NSSC19K0958** to CKS.